Supporting Information

Slow relaxation of magnetization for Tb derivative in a biradical-based lanthanide chain

Xiaochun Deng, Shuqi Ma, Mei Zhu,* Li Zhang,* and Yaohong Lv

Department of Chemistry, Zhejiang Sci-Tech University, Hangzhou 310018, China

1. X-ray Crystallography

2. Magnetic measurements

Table S1 Selected bond lengths [Å] and angles [°] for complex **1**, **2**

Complex **1**		Complex **2**	
Y(1)–O(1)	2.343(4)	Gd(1)-O(1)	2.391(4)
Y(1)–O(2)	2.323(4)	Gd(1)-O(2)	2.373(4)
Y(1)–O(3)	2.336(4)	Gd(1)-O(3)	2.376(4)
Y(1)–O(4)	2.336(4)	Gd(1)-O(5)	2.355(4)
O(4)-Y(1)-O(1)	73.62(14)	O(5)-Gd(1)-O(1)	104.96(13)
O(4)-Y(1)-O(2)	105.28(14)	O(5)-Gd(1)-O(2)	103.72(18)
O(4)-Y(1)-O(3)	74.47(14)	O(5)-Gd(1)-O(3)	79.92(17)
O(4)#1-Y(1)-O(1)	150.93(16)	O(5)#1-Gd(1)-O(1)	150.54(14)
O(4)#1-Y(1)-O(2)	90.89(14)	O(5)#1-Gd(1)-O(2)	91.64(14)
O(4)#1-Y(1)-O(3)	70.09(14)	O(5)#1-Gd(1)-O(3)	70.24(14)
O(4)-Y(1)-O(4)#1	135.1(2)	O(5)#1-Gd(1)-O(5)	135.31(19)
N(2)-O(4)-Y(1)	137.4(4)	N(1)-O(5)-Gd(1)	122.5(4)

Table S2 Selected bond lengths [Å] and angles [°] for complex **3**, **4**

Complex **3**		Complex **4**	
Tb(1)–O(1)	2.363(6)	Dy(1)-O(1)	2.351(3)
Tb(1)–O(2)	2.345(6)	Dy(1)-O(2)	2.341(3)
Tb(1)–O(3)	2.351(6)	Dy(1)-O(3)	2.343(2)
Tb(1)–O(4)	2.352(5)	Dy(1)-O(5)	2.342(2)
O(4)-Tb(1)-O(1)	74.10(19)	O(1)-Dy(1)-O(4)	150.48(10)
O(4)-Tb(1)-O(2)	105.1(2)	O(2)-Dy(1)-O(4)	90.48(9)
O(4)-Tb(1)-O(3)	74.1(2)	O(4)-Dy(1)-O(3)	69.88(9)
O(4)#2-Tb(1)-O(1)	150.4(2)	O(1)-Dy(1)-O(4)#1	74.28(10)
O(4)#2-Tb(1)-O(2)	91.5(2)	O(2)-Dy(1)-O(4)#1	105.85(9)
O(4)#2-Tb(1)-O(3)	70.3(2)	O(3)-Dy(1)-O(4)#1	74.57(9)
O(4)-Tb(1)-O(4)#2	135.1(3)	O(4)-Dy(1)-O(4)#1	134.84(13)
N(1)-O(4)-Tb(1)	135.9(5)	N(1)-O(4)-Dy(1)	136.3(2)

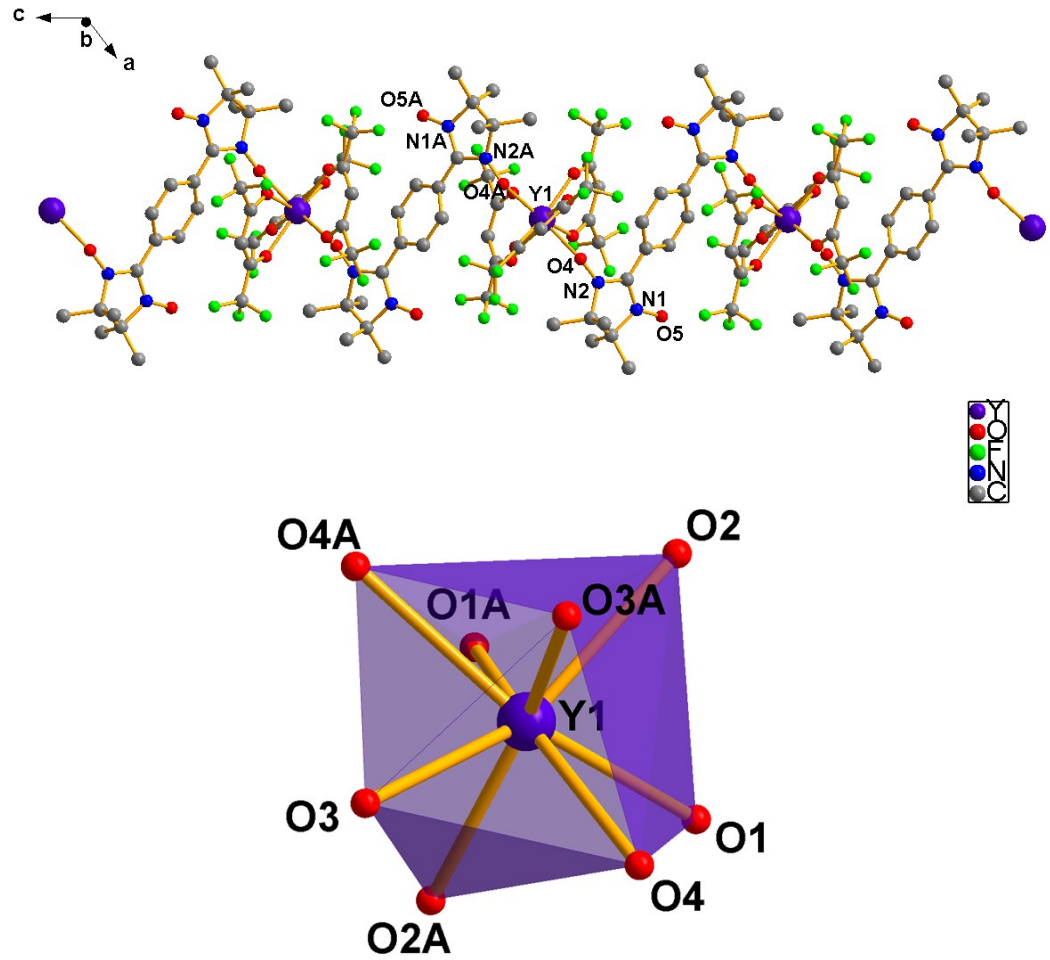

Fig. S1 (top) Crystal structure of complex **1** (H atoms are omitted for clarity and symmetry transformations used to generate equivalent atoms A: x, 1-y, 1/2+z); (bottom) Coordination polyhedrons of the Y(III) ion

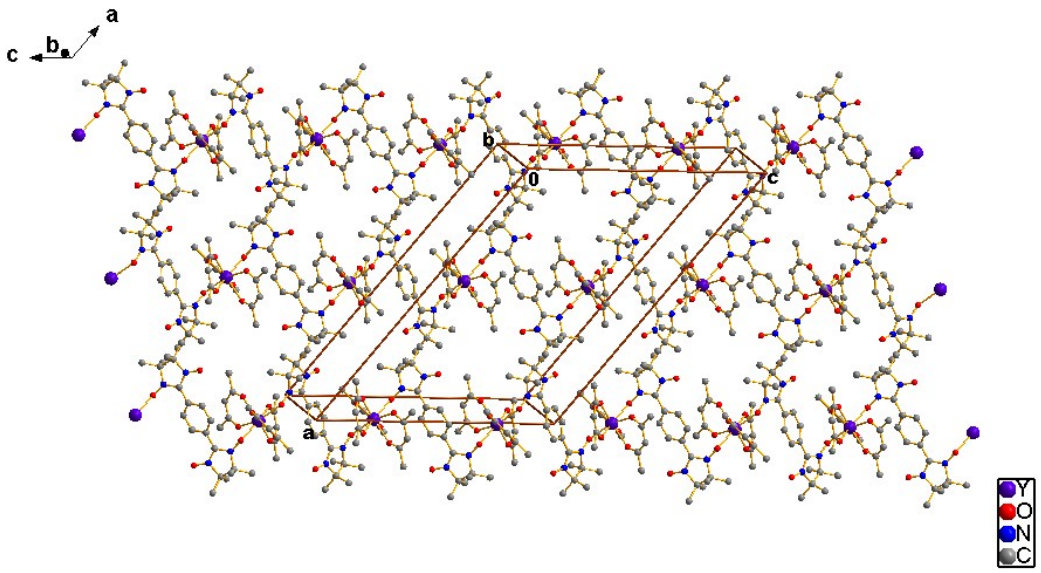

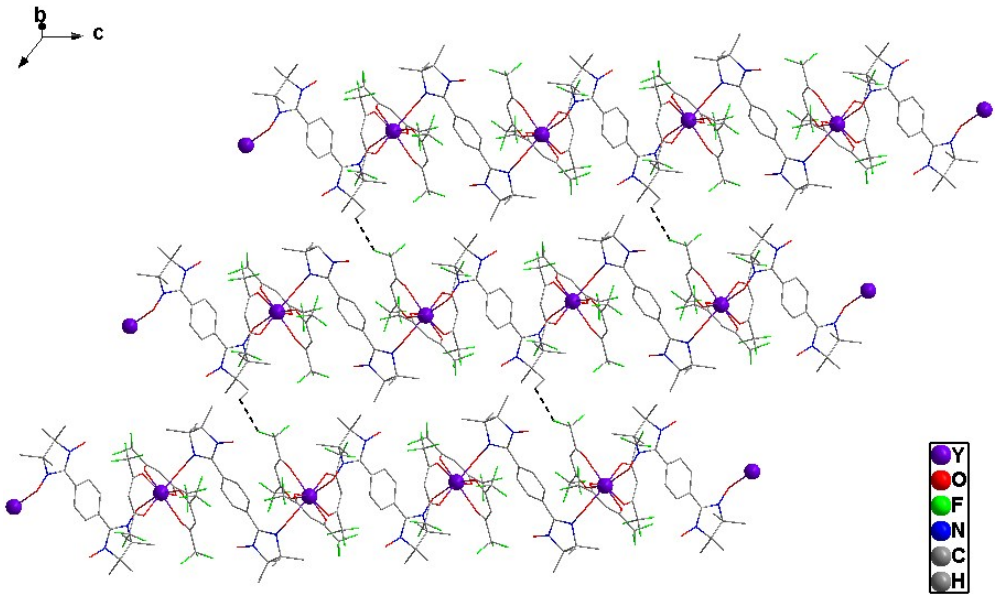

Fig. S2 (top) Packing diagram of complex **1**. (bottom) 2-D packing diagram of **1** through the weak intermolecular interactions: C2-H2C…F7 with the distance of 2.88 Å.

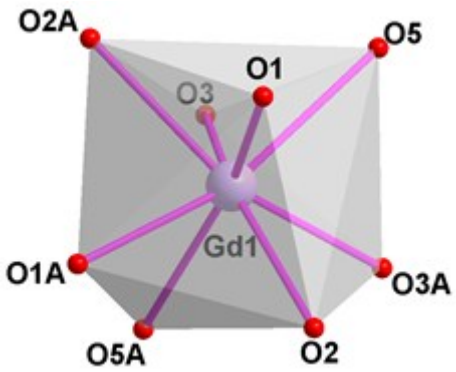

Fig. S3 Coordination polyhedrons of the Gd(III) ion

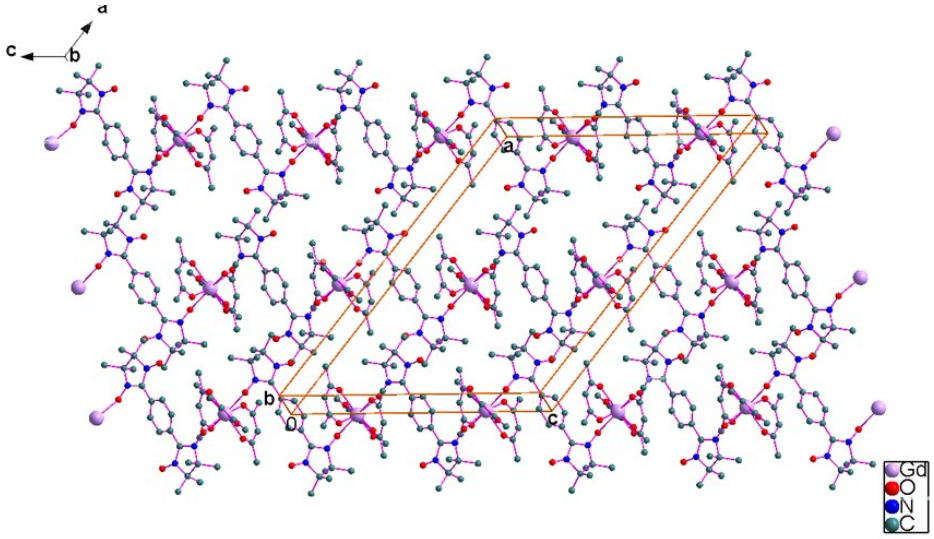

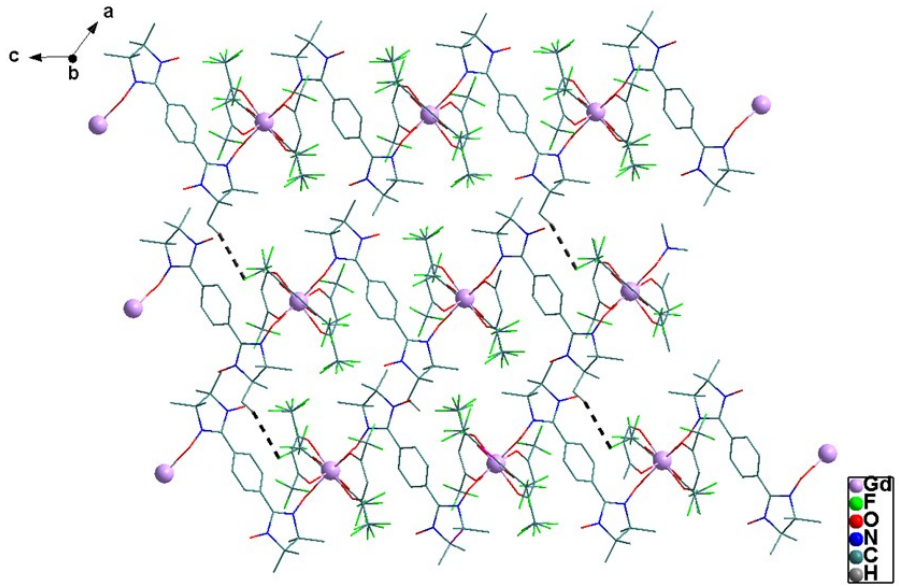

Fig. S4 (top) Packing diagram of complex **2**; (bottom) 2-D packing diagram of **2** through the weak intermolecular interactions: C16-H16B…F9 with the distance of 3.13 Å.

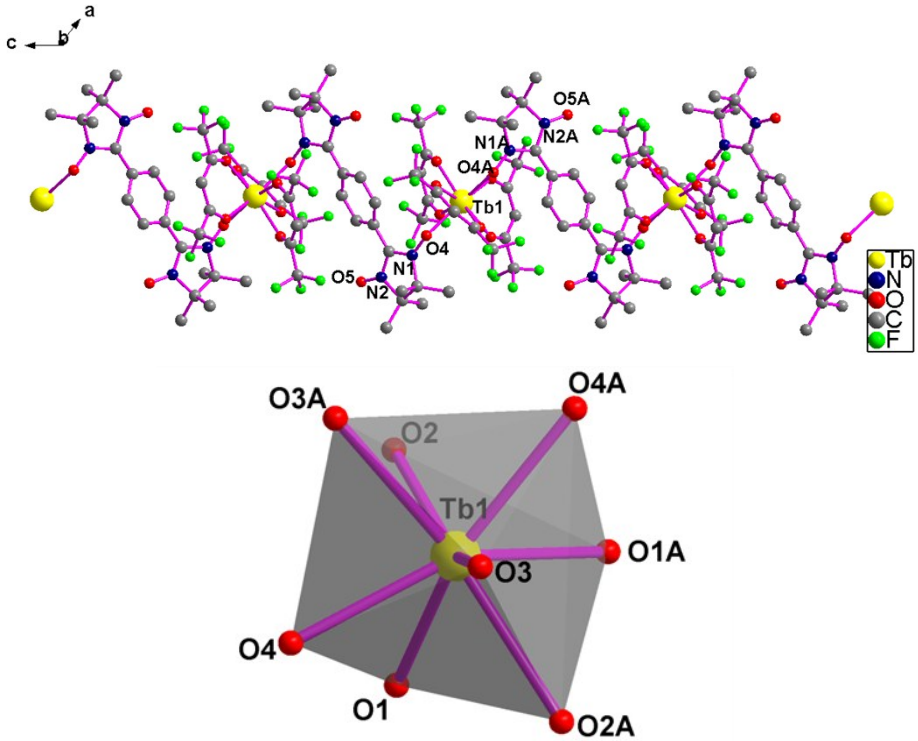

Fig. S5 (top) Crystal structure of complex **3** (H atoms are omitted for clarity and symmetry transformations used to generate equivalent atoms A: -x+1,y,-z+1/2); (bottom) Coordination polyhedrons of the Tb(III) ion.

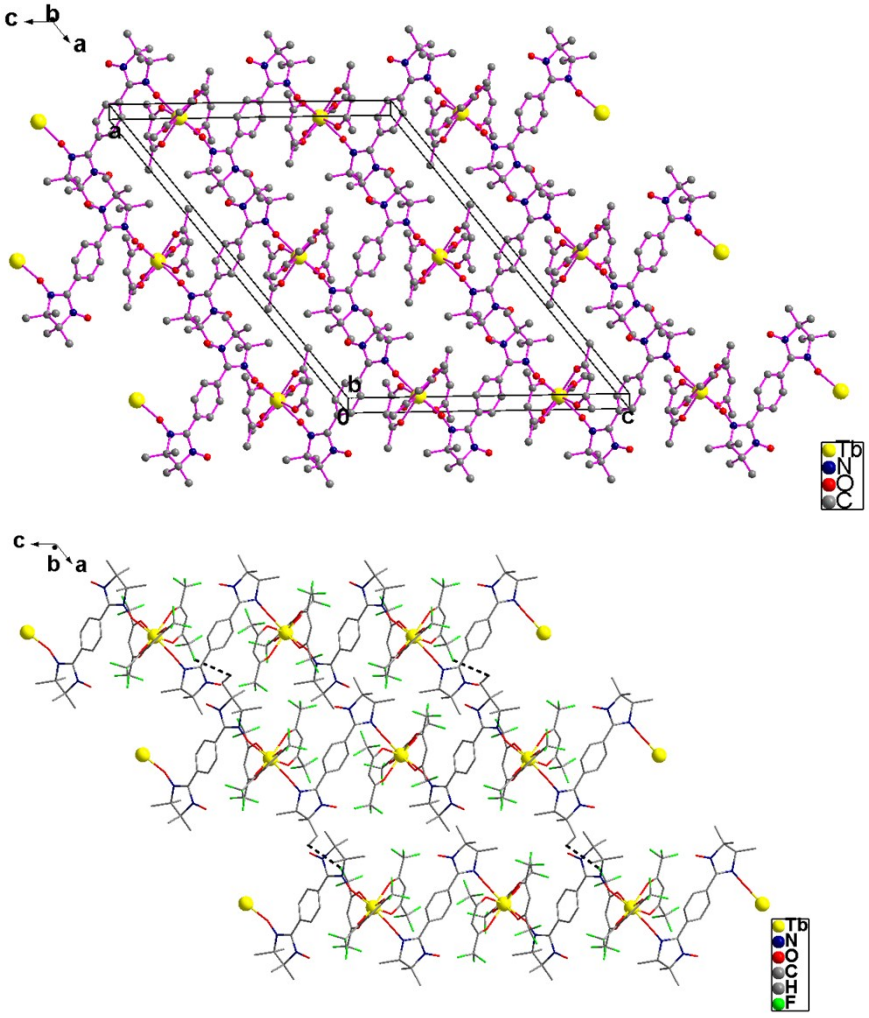

Fig. S6 (top) Packing diagram of complex **3**; (bottom) 2-D packing diagram of **3** through the weak intermolecular interactions: C16-H16B···F5#1 with the distance of 3.317 Å.

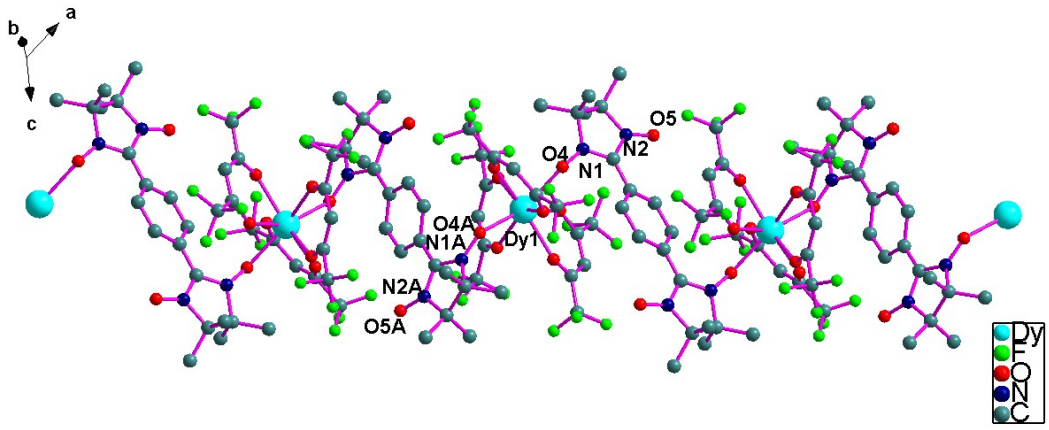

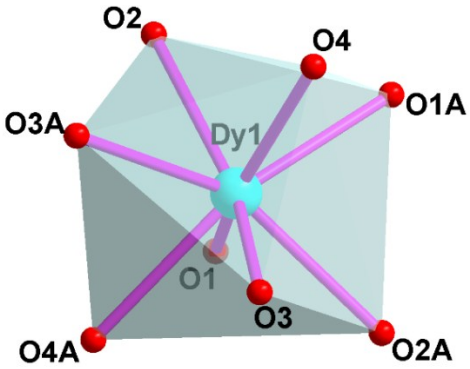

Fig. S7 (top) Crystal structure of complex **4** (H atoms are omitted for clarity and symmetry transformations used to generate equivalent atoms A: -x+1,y,-z+3/2); (bottom) The coordination polyhedron of Dy(III) ion.

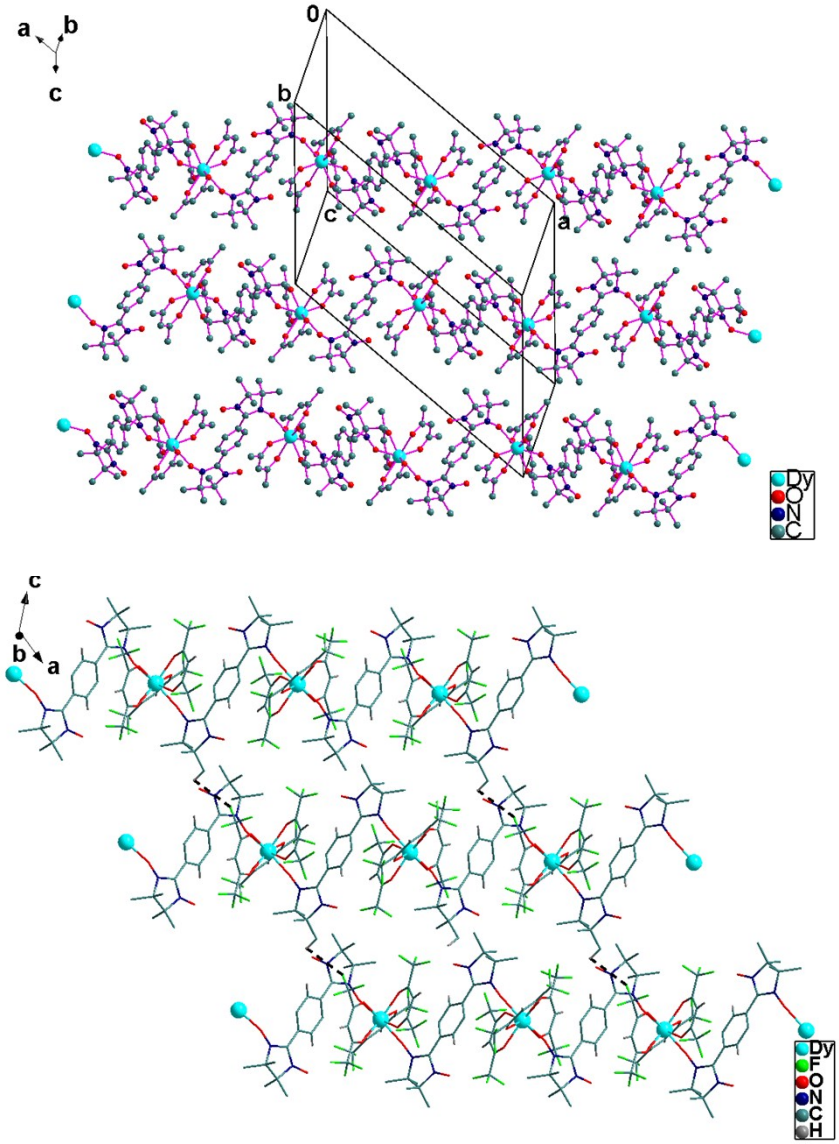

Fig. S8 (top) Packing of the chains in crystal for complex **4**; (bottom) 2D packing diagram of **4** through the weak intermolecular interactions: C18-H18C···F1 with the distance of 3.39 Å.

Table S3.Lanthanide geometry analysis by using the Shape software for complexes **1-4**.

Complex	Ln	D_{4d} SAPR	*Oh* CU	C_{2v} JBTPR
1	Y	**0.518**	1.235	2.219
2	Gd	**0.474**	1.327	2.231
3	Tb	**0.461**	1.309	2.210
4	Dy	**0.569**	1.148	2.182

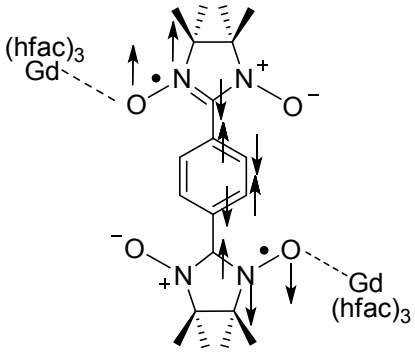

Scheme S1 Spin polarization mechanism for the magnetic coupling mediated by *p*-phenylene ring between two radicals.

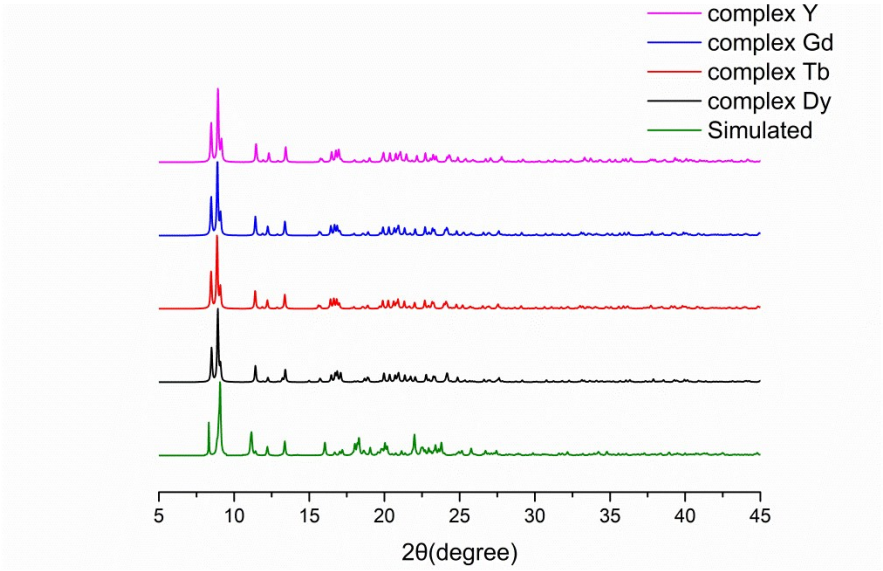

Fig. S9 Powder X-ray diffraction patterns of complexes **1-4**.

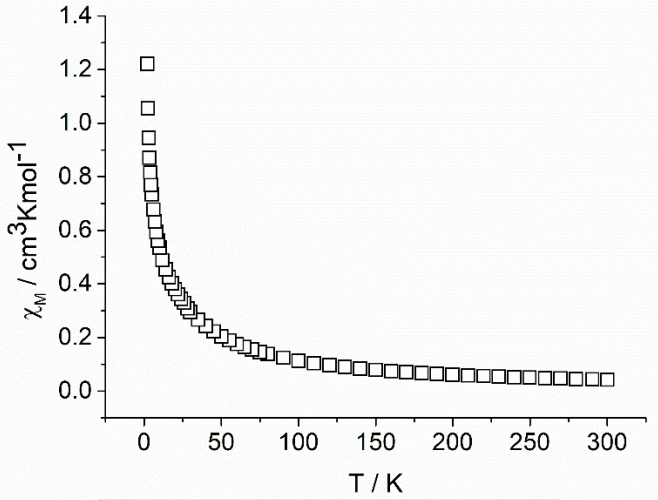

Fig. S10 χ_M versus T plot of complex **3**

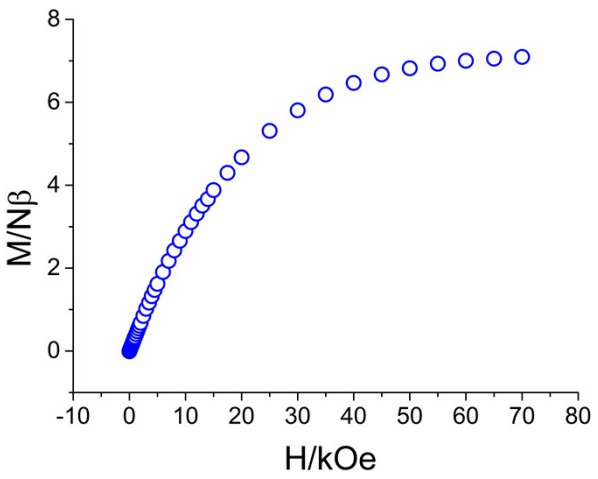

Fig. S11 Field dependent magnetization of complex **2** at 2K.

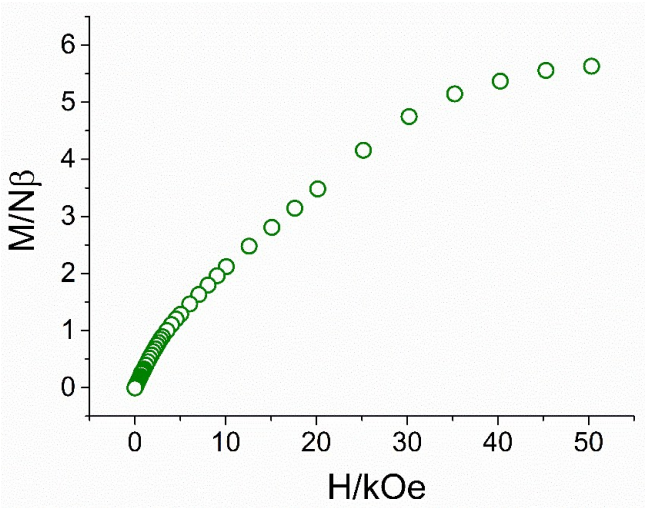

Fig. S12 Field dependent magnetization of complex **3** at 2K.

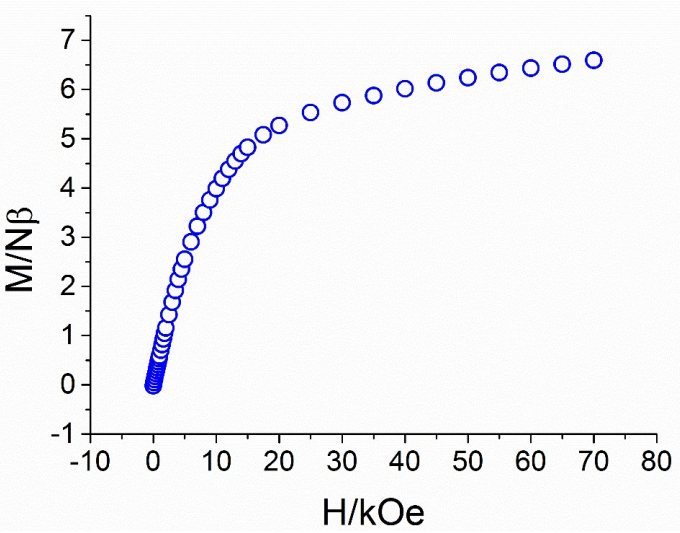

Fig. S13 Field dependent magnetization of complex **4** at 2K.

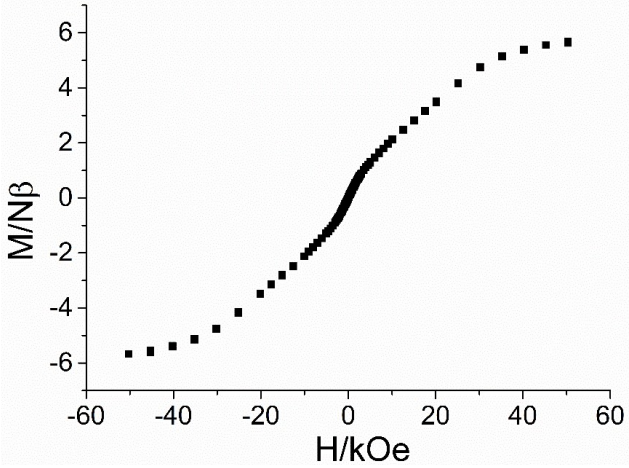

Fig. S14 *M vs H* behavior for **3** at 2 K recorded from 50 kOe to -50 kOe and back.

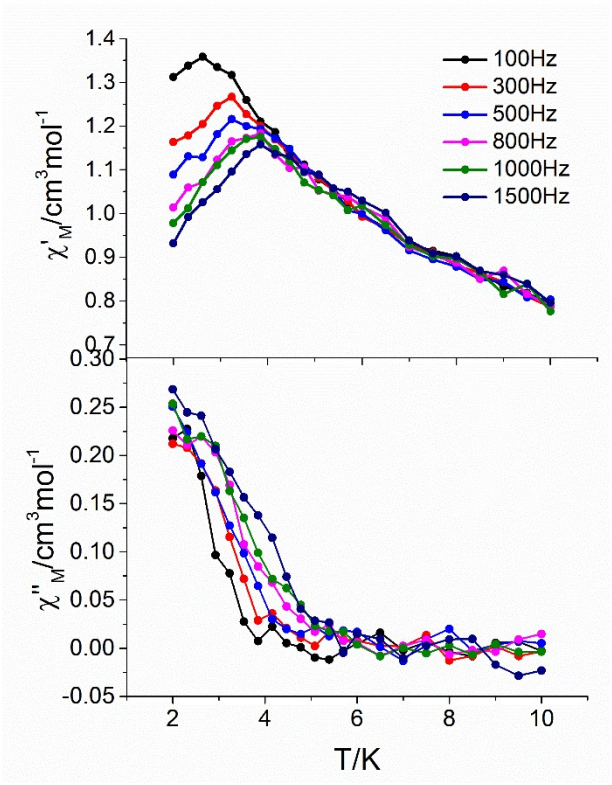

Fig. S15 Temperature dependence of the in-phase and out-of-phase components of the ac magnetic susceptibility for **3** in zero dc fields with an oscillation of 3.5 Oe.

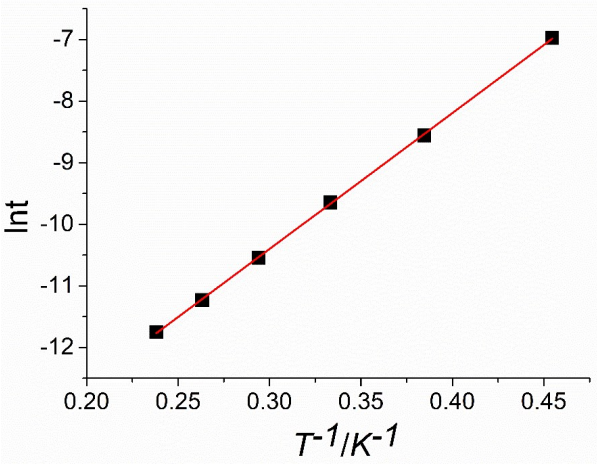

Fig. S16 Plots of lnτ versus T^{-1} fitting to the Arrhenius law for complex **3**.

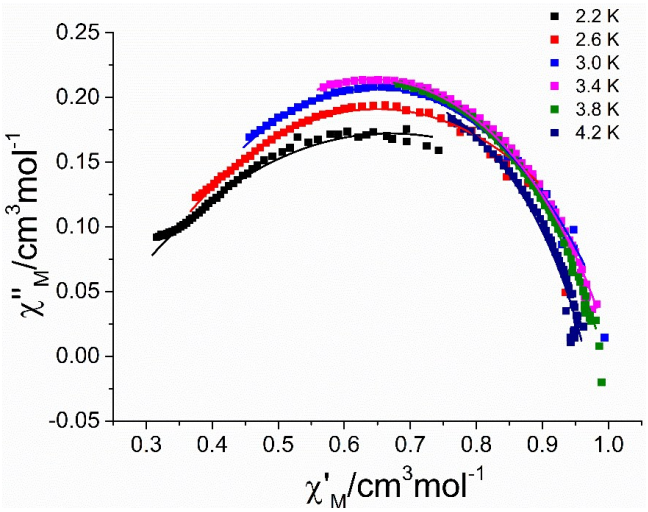

Fig. S17 Cole–Cole plots for complex **3** (The solid lines represent the fitting result).

Table S4 Best fitted parameters (χ_T, χ_S, τ and α) with the extended Debye model for complex **3** under 5000 dc field in the temperature range 2.2–4.2 K.

T/K	χ_S /cm^{3}mol^{-1}	χ_T /cm^{3}mol^{-1}	τ/s	α	R
2.2	0.19533	1.14459	9.34×10^{-4}	0.5568	2.28×10^{-3}
2.6	0.24836	1.03602	1.92×10^{-4}	0.42412	3.44×10^{-3}
3.0	0.26858	1.01861	6.27×10^{-5}	0.35749	5.69×10^{-3}
3.4	0.27638	1.00583	2.63×10^{-5}	0.32409	9.68×10^{-4}
3.8	0.29554	0.9929	1.33×10^{-5}	0.30361	2.85×10^{-3}
4.2	0.32548	0.96499	7.90×10^{-6}	0.27185	2.81×10^{-3}

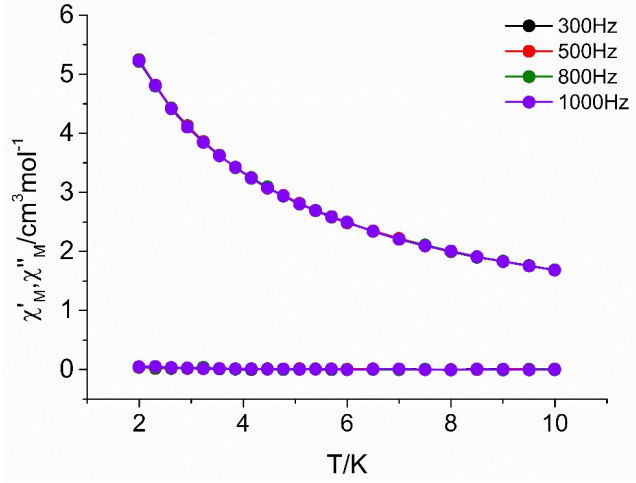

Fig. S18 Thermal dependence of the in-phase and out-of-phase susceptibility components for compound **4** at zero direct current (dc) field with an oscillation of 3 Oe.

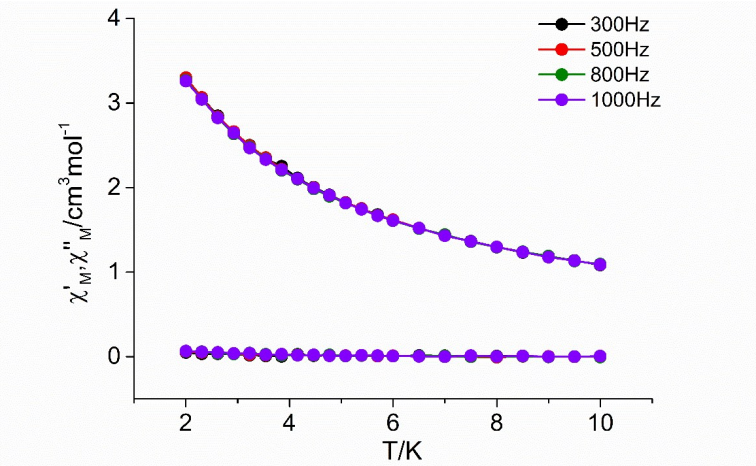

Fig. S19 Thermal dependence of the in-phase and out-of-phase susceptibility components for compound **4** at 1000 Oe dc field with an oscillation of 3 Oe.

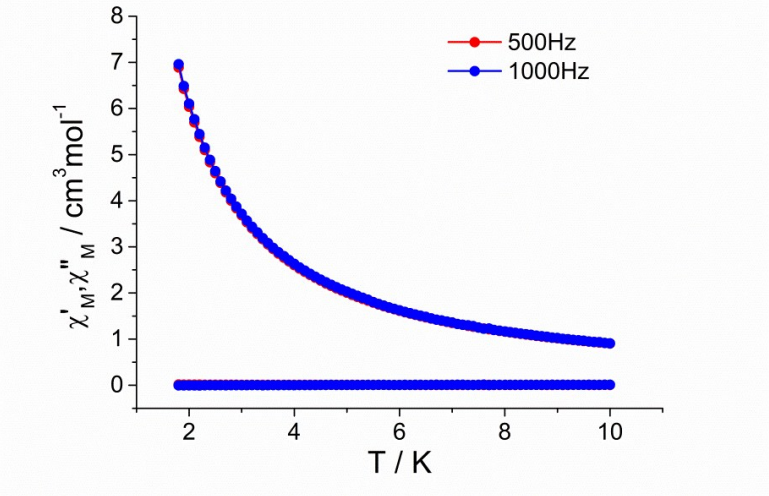

Fig. S20 Thermal dependence of the in-phase and out-of-phase susceptibility components for compound **2** at zero direct current (dc) field with an oscillation of 3 Oe.